

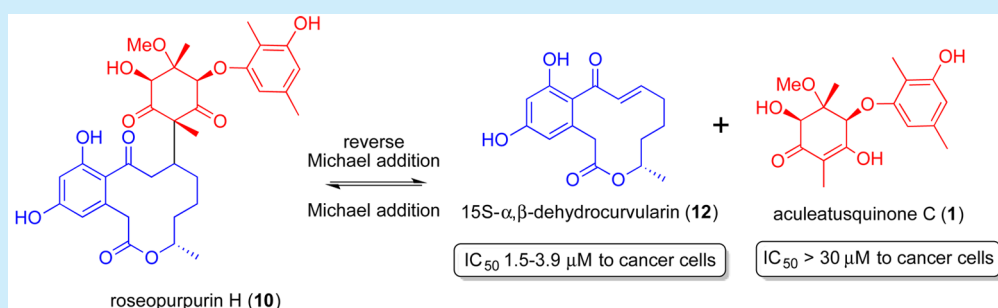
# Roseopurpurins: Chemical Diversity Enhanced by Convergent Biosynthesis and Forward and Reverse Michael Additions

Zhuo Shang,<sup>†</sup> Zeinab Khalil,<sup>†</sup> Li Li,<sup>‡</sup> Angela A. Salim,<sup>†</sup> Michelle Quezada,<sup>†</sup> Pabasara Kalansuriya,<sup>†</sup> and Robert J. Capon<sup>\*,†</sup>

<sup>†</sup>Institute for Molecular Bioscience, The University of Queensland, St. Lucia, QLD 4072, Australia

<sup>‡</sup>Beijing Key Laboratory of Active Substances Discovery and Druggability Evaluation, Institute of Materia Medica, Chinese Academy of Medical Sciences & Peking Union Medical College, Beijing 100050, China

## Supporting Information



**ABSTRACT:** Cultures of the estuarine fungus *Penicillium roseopurpureum* (CMB-MF038) yielded a diverse array of polyketides, many of which were related via a highly convergent biosynthetic pathway. In addition to revising and assigning structures, and documenting chemical and biological properties, pro-drug cytotoxic properties were attributed to roseopurpurins H (10) and I (11) on the basis of *in situ* reverse Michael addition to a cytotoxic Michael acceptor (12).

In recent years, marine-derived fungi have emerged as a valuable source of structurally diverse bioactive secondary metabolites. Our investigations, for example, have documented multidrug resistant antibacterial viridicatumtoxins and cytotoxic chaunolidones from mollusk-derived *Paecilomyces*<sup>1</sup> and *Chaunopycnis*,<sup>2</sup> antimycobacterial sydowiols and brevianamides from sediment-derived *Aspergillus sydowii*<sup>3</sup> and *Aspergillus versicolor*,<sup>4</sup> and the P-glycoprotein inhibitor shornephine A from a marine sediment-derived *Aspergillus* sp.<sup>5</sup>

We now report on a diverse array of polyketides produced by *Penicillium roseopurpureum* (CMB-MF038), isolated from estuarine mud collected in the Boondall Wetlands Reserve, Qld, Australia. HPLC analysis of CMB-MF038 cultured on multiple media revealed extracts rich in chemical diversity, with cytotoxicity exhibited against human cancer cell lines. We describe spectroscopic and chemical analyses leading to the structure elucidation of 1–22 (Figures 1 and S66), with commentary on a plausible highly convergent biosynthetic relationship. In documenting antibiotic and cytotoxic properties, we reveal 10 and 11 as rare examples of natural Michael adduct pro-drugs, being surrogates of the cytotoxic Michael acceptor 12.

Chemical fractionation of a rice cultivation of CMB-MF038 yielded the known (albeit rare) aculeatusquinones C–B (1–2) and the new biosynthetically related roseopurpurins A–I (3–11), together with known fungal metabolites 15S- $\alpha,\beta$ -dehydrocurvularin (12),<sup>6</sup> sumalarin C (13),<sup>7</sup> 12-oxocurvularin

(14),<sup>8</sup> citreofuran (15),<sup>8</sup> carviolin (16),<sup>9</sup> 6-chloro-carviolin (17),<sup>10</sup> carviolin-3-carboxylic acid (18),<sup>11</sup> 4-methylorcinol (19),<sup>12</sup> and 3-methyl-orsellinic acid (20).<sup>13</sup> By contrast, chemical fractionation of a 3.5% saline PYG agar cultivation of CMB-MF038 yielded citridone B/B' (21)<sup>14</sup> and citridone A (22).<sup>14</sup> The structure elucidation of 12–22 was achieved by spectroscopic analysis with reference to the scientific literature (see Supporting Information), while the structure elucidation of 1–11 is presented below.

HRESI(+)-MS analysis of 1 returned a *quasi*-molecular ion ( $[M + Na]^+$ ) consistent with a molecular formula ( $C_{17}H_{22}O_6$ ,  $\Delta m_{\text{mu}} -0.1$ ) requiring seven double bond equivalents (DBE). The <sup>13</sup>C NMR (MeOH-*d*<sub>4</sub>) data for 1 (Table S4) revealed resonances for an unsymmetrically pentasubstituted benzene and three additional sp<sup>2</sup> quaternary carbons, accounting for six DBE, with the remaining DBE attributed to a ring. Consideration of diagnostic 2D NMR correlations (Figure S64) suggested 1 was the known metabolite aculeatusquinone C, first reported in 2013 by Chen et al. from an estuarine sediment-derived *Aspergillus aculeatus*.<sup>15</sup> Supportive of this assignment, the 1D NMR (MeOH-*d*<sub>4</sub>) data for 1 were an excellent match with those reported for aculeatusquinone C.<sup>15</sup> Similarly, the minor cometabolite 2 ( $C_{17}H_{20}O_6$ ,  $\Delta m_{\text{mu}} -0.2$ ) (Table S5) was identified as aculeatusquinone B (2), previously

Received: July 18, 2016

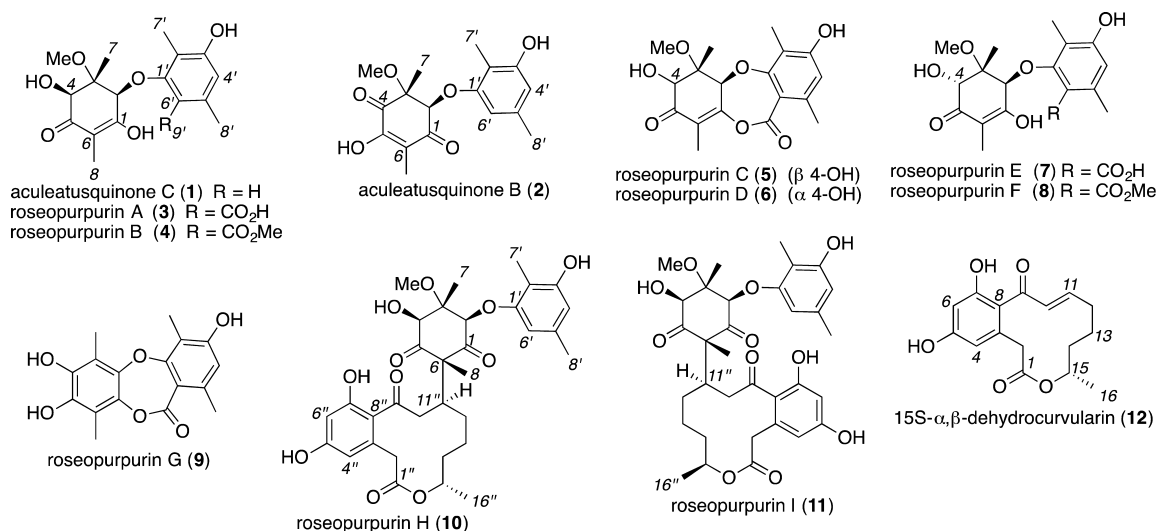


**Figure 1.** *Penicillium roseopurpureum* (CMB-MF038) metabolites.

reported as a cometabolite of **1**.<sup>15</sup> Consistent with the 2013 report, relative configurations were assigned to **1** and **2** based on ROESY correlations between H-2, 3-OMe and H-4 (Figure S64). As published structures for **1–2** were limited to relative configurations, we assigned full configurations as shown below.

HRESI(+)-MS analysis of **3** returned a *quasi*-molecular ion ( $[M + Na]^+$ ) consistent with a molecular formula (C<sub>18</sub>H<sub>22</sub>O<sub>8</sub>, Δ<sub>mmu</sub> −0.6) for a carboxylated (+44 amu) analogue **1**, while **4** (C<sub>19</sub>H<sub>24</sub>O<sub>8</sub>, Δ<sub>mmu</sub> −0.5) was attributed to a methylated (+14 amu) homologue of **3**. Significantly, comparison of the 1D NMR (MeOH-*d*<sub>4</sub>) data for **3** (Table S6) with those for **1** revealed a near identical C-1 to C-8 moiety, with the only significant difference being the absence of an aromatic methine (δ<sub>H</sub> 6.30) and the presence of a carboxylic acid moiety (δ<sub>C</sub> 172.7). Similarly, comparison of the 1D NMR (MeOH-*d*<sub>4</sub>) data for **4** (Table S7) with those for **3** revealed the only significant difference as the appearance of a CO<sub>2</sub>Me moiety (δ<sub>H</sub> 3.76; δ<sub>C</sub> 52.6). Diagnostic 2D NMR correlations (Figure S64) were supportive of structures for roseopurpurins A (**3**) and B (**4**), albeit with the C-6' versus C-4' regiochemistry of the CO<sub>2</sub>H moiety in **3**, and CO<sub>2</sub>Me moiety in **4**, and relative configurations, resolved as detailed below.

The HRESI(+)-MS determined molecular formulas for the cometabolites **5** (C<sub>18</sub>H<sub>20</sub>O<sub>7</sub>, Δ<sub>mmu</sub> −0.3) and **6** (C<sub>18</sub>H<sub>20</sub>O<sub>7</sub>, Δ<sub>mmu</sub> +0.2) were strongly suggestive of isomeric dehydration analogues of **3**, with detailed analysis of 1D and 2D NMR (MeOH-*d*<sub>4</sub>) data (Tables S8 and S9, Figure S64) supporting lactonization across 6'-CO<sub>2</sub>H and 1-OH. Of note, sharper and more pronounced <sup>13</sup>C NMR resonances for C-1, C-5, and C-6 in **5** and **6** were consistent with lactonization to 1-OH and the loss of keto–enol tautomerization-mediated broadening. A 1997 patent described cytotoxic *Aspergillus* metabolites with planar structures in common with **5** and **6** (albeit without adequate spectroscopic characterization or structure proof).<sup>16</sup> In our hands, diagnostic ROESY correlations between H-2, 3-OMe, and H-4 established the relative configuration for roseopurpurin C (**5**) (Figure S64), while correlations between H-2 and 3-OMe, and H-4 and H<sub>3</sub>-7, established the C-4 epimeric relative configuration for roseopurpurin D (**6**) (Figure S64). Significantly, acid transformation of **5** yielded **1**, **3**, and **4** (Figure S7), unambiguously confirming structures and common relative configurations to **1–4**. By contrast, acid

transformation of **6** yielded products tentatively identified by LC-MS and mechanistic considerations as the C-4 epimers roseopurpurins E (**7**) and F (**8**), both of which were detected as minor cometabolites in the crude CMB-MF038 extract.

Having independently assigned structures with relative configurations to **1–8**, we turned our attention to absolute configurations. A comparison of <sup>1</sup>H NMR data for the C-4 *R*-MTPA and *S*-MTPA esters of **1** (a Mosher analysis) (Table S1) revealed diagnostic shielding of H-7 (Δδ<sub>S-R</sub> −97 Hz) consistent with a 2*S*, 3*S*, 4*S* configuration for **1** (Figure S3) and supportive of absolute configurations for **2–8** as indicated. These assignments were further confirmed by a comparison of experimental CD spectra for **5** and **6**, with calculated ECD spectra (time-dependent density functional theory, B3LYP/6-31g(d)) for the 2*S*, 3*S*, 4*S* and 2*R*, 3*R*, 4*R* enantiomers of **5** and 2*S*, 3*S*, 4*R* and 2*R*, 3*R*, 4*S* enantiomers of **6** (Figure S6).

HRESI(+)-MS analysis of **9** returned a *quasi*-molecular ion ( $[M + Na]^+$ ) indicative of a molecular formula (C<sub>17</sub>H<sub>16</sub>O<sub>6</sub>, Δ<sub>mmu</sub> +0.1) requiring 10 double bond equivalents (DBE), which 1D NMR (MeOH-*d*<sub>4</sub>) data (Table S10) attributed to a C-1' to C-9' dimethylresorcinol/lactone moiety in common with **5** and **6** and an aromatized fully substituted C-1 to C-6 residue. Diagnostic 2D NMR correlations (Figure S64) confirmed the structure for roseopurpurin G (**9**) as indicated.

HRESI(+)-MS analysis of **10** and **11** returned *quasi*-molecular ions ( $[M + Na]^+$ ) indicative of isomeric (C<sub>33</sub>H<sub>40</sub>O<sub>11</sub>, Δ<sub>mmu</sub> −0.1 and +0.4) Michael addition adducts between the known Michael acceptor **1** and a putative nucleophile derived from the cometabolite **1**. More specifically, the 1D NMR (MeOH-*d*<sub>4</sub>) data for **10** and **11** (Tables S11 and S12) revealed that main differences in resonances compared to **1** are replacement of the olefinic methyl in **1** (δ<sub>H</sub> 1.73, H<sub>3</sub>-8; δ<sub>C</sub> 7.7, C-8) with an aliphatic tertiary methyl in **10** (δ<sub>H</sub> 1.13, H<sub>3</sub>-8; δ<sub>C</sub> 11.1, C-8) and **11** (δ<sub>H</sub> 1.11, H<sub>3</sub>-8; δ<sub>C</sub> 11.4, C-8), indicative of C-6 alkyl addition. This addition was further evidenced by disruption of the tautomeric 1,3-diketone, enabling the ready detection of <sup>13</sup>C NMR ketone resonances in both **10** (δ<sub>C</sub> 205.8, C-1; 207.4, C-5) and **11** (δ<sub>C</sub> 205.2, C-1; 208.0, C-5). Further analysis of the 1D NMR data for **10** and **11** revealed resonances attributed to a Michael addition adduct of **12**. Significant differences in the 1D NMR data for **10** and **11** compared to **12** included replacement of the α,β-unsaturated ketone in **1** with a β-

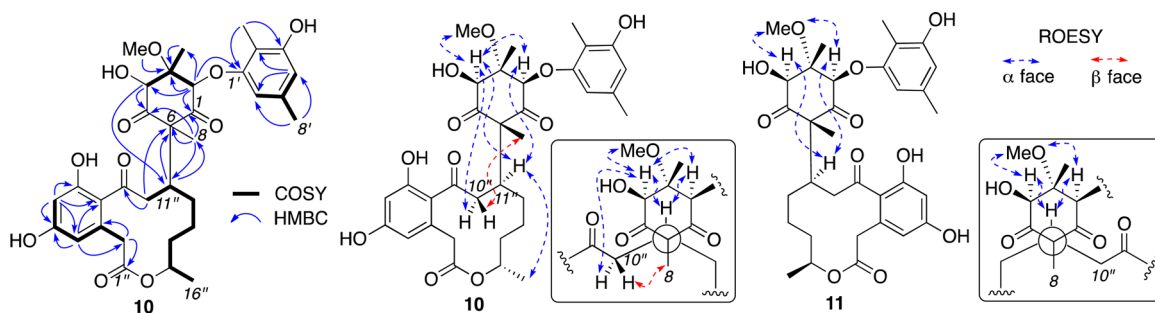


Figure 2. Diagnostic 2D NMR (MeOH- $d_4$ ) correlations for **10** and **11**.

substituted ketone in **10** and **11**. The structure assignments outlined above for **10** and **11** were further confirmed by diagnostic 2D NMR correlations (Figure 2). COSY and HMBC correlations for **10** (largely mirrored by **11**) defined three key structure fragments, namely C-1 to C-8, C-1' to C-8', and C-1'' to C-16''. Furthermore, HMBC correlations from H-2 to C-1', and H-11'' to C-6, permitted assembly of these fragments as indicated.

Diagnostic ROESY correlations for **10** and **11** (Figure 2), together with biosynthetic considerations (Figure 3), were

supportive of a C-2, C-3, C-4 absolute configuration in common with **1**. Significantly, both **10** and **11** exhibited ROESY correlations from H-11'' to H-2 and H-4, consistent with a 6R configuration, and a common  $\alpha$ -facial 2,4,6-triaxial configuration between H-2, H-4, and C-11'' (Figure 2). Furthermore, consideration of the lowest energy staggered conformation about the C-6 to C-11'' bond and a ROESY correlation from H-10''a to H-4 supported an 11''S configuration for **10**, and by inference an 11''R configuration for **11** (Figures 2 and S65). A 15''S configuration was assigned **10** and **11**, in common with the likely biosynthetic precursor and cometabolite **12**.

We propose a highly convergent biosynthetic relationship between **1–11** and **19–20**, which involves a common polyketide precursor that undergoes Aldol condensation-mediated transformation by three alternate pathways (Figure 3). Pathway A proceeds via concerted decarboxylation and dehydration to yield **19**, while pathway B employs a simple dehydration to yield **20**. Pathway C proceeds through initial methylation of the 3-OH moiety, blocking dehydration-mediated transformation via pathways A and B. Subsequent keto–enol mediated decarboxylation and oxidation yields a key intermediate (ii). This intermediate (ii) undergoes a stereo-selective ( $\beta$ -facial) extended Michael addition by the cometabolite **19** to yield **1**, with subsequent C-4 oxidation returning **2**. Likewise, an alternate extended Michael addition to (ii) by the cometabolite **20** yields the C-4 epimers **3** and **7**, which can be readily transformed to the methyl esters **4** and **8**, and the lactones **5** and **6**, respectively. Finally, deprotonation of **1** can yield the cyclohexandione enolate anion (iii) which engages in a *pseudo*-axial C-6 nucleophilic Michael addition to C-11'' in the Michael acceptor cometabolite **12**, with *si*-facial addition yielding the 11''S adduct **10**, and *re*-facial addition yielding the 11''R adduct **11**. We propose that the adducts **10** and **11** are natural products (not handling artifacts) as they were detected in the crude cultivation extracts (Figure S1), and in our hands could not be generated by either acid, base, or heat treatment of a mixture of **1** and **12**.

None of the metabolites **1–6** and **9–12** exhibited growth inhibitory activity against a panel of Gram-positive or Gram-negative bacteria (Table S2) ( $IC_{50} > 30 \mu M$ ). Likewise **1–4** and **9** were noncytotoxic ( $IC_{50} > 30 \mu M$ ), and lactones **5** and **6** exhibited only modest cytotoxicity ( $IC_{50}$  3.9–28.4  $\mu M$ ), toward human colon (SW620), lung (NCI-H460), cervix (KB3-1), and hepatocellular (HepG2) carcinoma cells. By contrast, significant levels of cytotoxicity were observed for **10** ( $IC_{50}$  1.5–3.9  $\mu M$ ), **11** ( $IC_{50}$  1.8–8.4  $\mu M$ ), and **12** ( $IC_{50}$  1.9–10.2  $\mu M$ ) (Table 1).

Given the absence of a highly reactive Michael acceptor moiety, we were surprised at the cytotoxicity exhibited by **10** and **11**. To explain this anomaly, we speculated that **10** and **11**

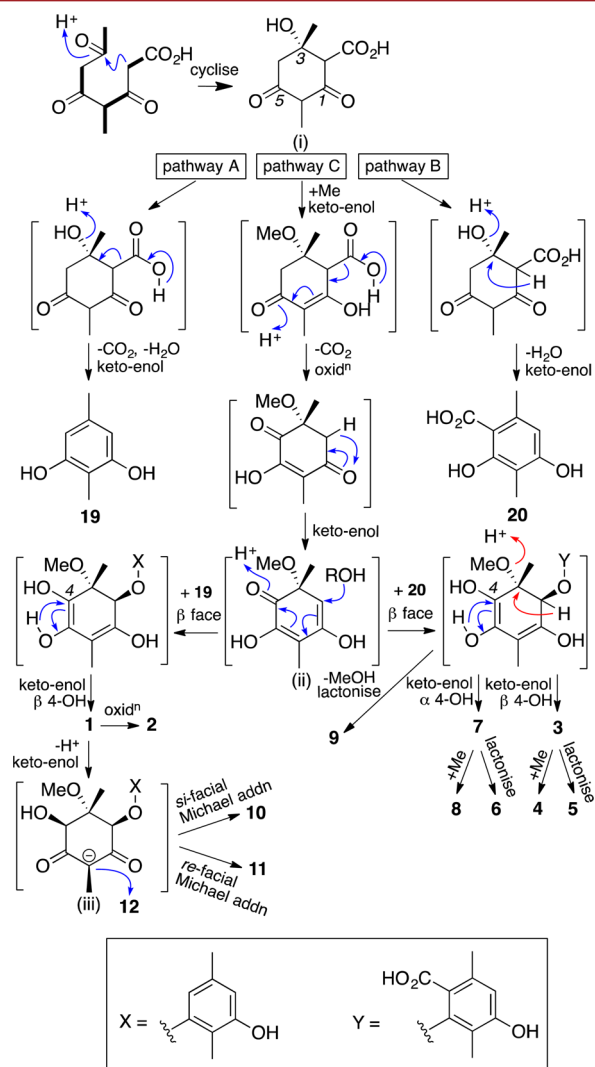


Figure 3. Plausible convergent biosynthetic relationships.

Table 1. Cytotoxic Activities ( $IC_{50}$ ,  $\mu M$ ) of 5–6 and 9–12

cell line <sup>a</sup>	5	6	9	10	11	12
SW620	3.9	5.0	25.3	1.5	2.8	1.9
NCI-H460	10.0	4.7	>30	1.6	1.8	3.7
KB3-1	18.4	17.3	>30	2.0	3.6	4.0
HepG2	28.4	18.7	>30	3.9	8.4	10.2

<sup>a</sup>Human carcinomas: SW620, colon; NCI-H460, lung; KB3-1, cervix; and HepG2, hepatocellular.

were prone to reverse Michael addition to yield **12** as the actual cytotoxic agent (Figure 4). To test this hypothesis we

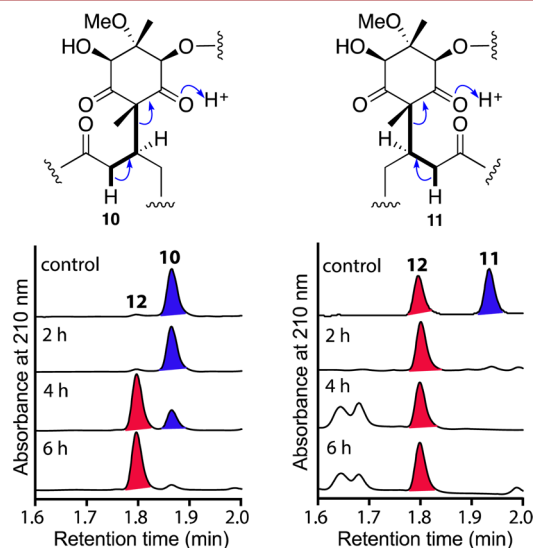


Figure 4. Time study of reverse Michael addition of **10** and **11** in NCI-H460 cells. Control: compound incubated in media only for 36 h.

performed a time course study on SW620 and NCI-H460 cells exposed to **10** or **11** ( $10 \mu M$ ). As we predicted, these analyses revealed that **10** and **11** underwent reverse Michael addition to yield **12**, albeit at differing rates. Whereas **10** was unaffected, **11** exhibited significant ( $\sim 50\%$ ) conversion to **12** after 36 h of exposure to culture media alone (Figure 4). Likewise, in the presence of cancers cells, **10** and **11** underwent quantitative conversion to **12** in 6 and  $<2$  h, respectively (Figures 4, S10, and S11). The differing chemical/enzymatic reverse Michael addition proclivity of **10** and **11** likely reflects the ease with which they attain the requisite *trans*-antiparallel transitional state.

In conclusion, structures inclusive of absolute configurations (where applicable) were assigned to **1–22** on the basis of detailed spectroscopic analysis, chemical derivatization, calculated ECD, and biosynthetic considerations. The chemical diversity observed in **1–11** is evidence of a highly convergent Michael addition enabled biosynthetic relationship. The Michael adducts **10** and **11** are rare examples of natural product *pro*-drugs, undergoing *in situ* reverse Michael addition to yield the cytotoxic Michael acceptor **12**. This latter transformation suggests an intriguing natural product-inspired strategy for enhancing the therapeutic potential of bioactive Michael acceptors, by masking them as enzyme-activated, reversible Michael adducts with suitably substituted cyclohexandiones (e.g., Meldrum's acid, dimedone).

## ■ ASSOCIATED CONTENT

### Supporting Information

The Supporting Information is available free of charge on the ACS Publications website at DOI: 10.1021/acs.orglett.6b02099.

General experimental procedures, spectroscopic data, taxonomy of *P. roseopurpureum* (CMB-MF038), and biological assay (PDF)

## ■ AUTHOR INFORMATION

### Corresponding Author

\*E-mail: r.capon@uq.edu.au.

### Notes

The authors declare no competing financial interest.

## ■ ACKNOWLEDGMENTS

This research was funded in part by the Institute for Molecular Bioscience, UQ, and the Australian Research Council (DP120100183). Z.S. acknowledges UQ for an International Postgraduate Research Scholarship.

## ■ REFERENCES

- (1) Shang, Z.; Salim, A. A.; Khalil, Z. G.; Quezada, M.; Bernhardt, P. V.; Capon, R. J. *J. Org. Chem.* **2015**, *80*, 12501.
- (2) Shang, Z.; Li, L.; Espósito, B. P.; Salim, A. A.; Khalil, Z. G.; Quezada, M.; Bernhardt, P. V.; Capon, R. J. *Org. Biomol. Chem.* **2015**, *13*, 7795.
- (3) Liu, X.; Song, F.; Ma, L.; Chen, C.; Xiao, X.; Ren, B.; Liu, X.; Dai, H.; Piggott, A. M.; Av-Gay, Y.; Zhang, L.; Capon, R. J. *Tetrahedron Lett.* **2013**, *54*, 6081.
- (4) Song, F.; Liu, X.; Guo, H.; Ren, B.; Chen, C.; Piggott, A. M.; Yu, K.; Gao, H.; Wang, Q.; Liu, M.; Liu, X.; Dai, H.; Zhang, L.; Capon, R. J. *Org. Lett.* **2012**, *14*, 4770.
- (5) Khalil, Z. G.; Huang, X. C.; Raju, R.; Piggott, A. M.; Capon, R. J. *Org. Chem.* **2014**, *79*, 8700.
- (6) (a) Almassi, F.; Ghisalbetti, E. L.; Skelton, B. W.; White, A. H. *Aust. J. Chem.* **1994**, *47*, 1193. (b) Greve, H.; Schupp, P. J.; Eguereva, E.; Kehraus, S.; Kelter, G.; Maier, A.; Fiebig, H. H.; König, G. M. *Eur. J. Org. Chem.* **2008**, *2008*, 5085.
- (7) Meng, L. H.; Li, X. M.; Lv, C. T.; Li, C. S.; Xu, G. M.; Huang, C. G.; Wang, B. G. *J. Nat. Prod.* **2013**, *76*, 2145.
- (8) Lai, S.; Shizuri, Y.; Yamamura, S.; Kawai, K.; Terada, Y.; Furukawa, H. *Tetrahedron Lett.* **1989**, *30*, 2241.
- (9) Eilbert, F.; Anke, H.; Sterner, O. *J. Antibiot.* **2000**, *53*, 1123.
- (10) Cohen, P. A.; Neil Towers, G. H. *Phytochemistry* **1996**, *42*, 1325.
- (11) Haggerty, T. J.; Kurnick, J. T.; Dunn, I. S. (Cytocure Llc), WO2012166617A2, 2012.
- (12) Guo, J.; Li, Z. L.; Wang, A. L.; Liu, X. Q.; Wang, J.; Guo, X.; Jing, Y. K.; Hua, H. M. *Planta Med.* **2011**, *77*, 2042.
- (13) Nagumo, S.; Ishizawa, S.; Nagai, M.; Inoue, T. *Chem. Pharm. Bull.* **1996**, *44*, 1086.
- (14) Fukuda, T.; Tomoda, H.; Omura, S. *J. Antibiot.* **2005**, *58*, 315.
- (15) Chen, L.; Zhang, W.; Zheng, Q.; Liu, Q.; Zhong, P.; Hu, X.; Fang, Z.; Zhang, Q. *Heterocycles* **2013**, *87*, 861.
- (16) Dhingra, U. H.; Shirai, H.; Takehana, Y.; Wovkulich, P. M.; Yabuki, N. (F. Hoffmann-La Roche Ag), WO 9747611A1, 1997.